Mathematical optimization of procedures for cryoprotectant equilibration using a toxicity cost function ☆

James D. Benson [a,1], Anthony J. Kearsley [a], Adam Z. Higgins [b,*]

[a] *Applied and Computational Mathematics Division, National Institute of Standards and Technology, Gaithersburg, MD 20899, USA*
[b] *School of Chemical, Biological and Environmental Engineering, Oregon State University, Corvallis, OR 97331-2702, USA*

ABSTRACT

Cryopreservation nearly universally depends on the equilibration of cells and tissues with high concentrations of permeating chemicals known as cryoprotective agents, or CPAs. Despite their protective properties, CPAs can cause damage as a result of osmotically-driven cell volume changes, as well as chemical toxicity. In this study, we have used previously published data to determine a toxicity cost function, a quantity that represents the cumulative damage caused by toxicity. We then used this cost function to define and numerically solve the optimal control problem for CPA equilibration, using human oocytes as representative cell type with high clinical relevance. The resulting toxicity-optimal procedures are predicted to yield significantly less toxicity than conventional stepwise procedures. In particular, our results show that toxicity is minimized during CPA addition by inducing the cell to swell to its maximum tolerable volume and then loading it with CPA while in the swollen state. This counterintuitive result is considerably different from the conventional stepwise strategy, which involves exposure to successively higher CPA concentrations in order to avoid excessive shrinkage. The procedures identified in the present study have the potential to significantly reduce damage due to toxicity and warrant further investigation.

© 2012 Elsevier Inc. All rights reserved.

Introduction

Stabilization of viable cells by cryopreservation is important in several areas, including cell-based therapy, tissue engineering and transplantation medicine. In particular, human oocyte cryopreservation has been the subject of intense research in the past decade because of its importance in *in vitro* fertilization [3,5,23,24,28,29,38]. The ability to successfully cryopreserve human oocytes would obviate the need for cryo-storage of human embryos, a practice that is ethically controversial and even illegal in some countries [3]. Moreover, the ability to cryopreserve oocytes would expand the fertility options for women at risk for losing ovarian function (e.g., women undergoing chemotherapy), and for women who may wish to delay having children until a later time [3,24].

There are two fundamental cryopreservation strategies – conventional freezing (also called equilibrium or slow freezing) and vitrification – and both involve the use of cryoprotective agents (CPAs) such as ethylene glycol or dimethyl sulfoxide (Me$_2$SO). With conventional freezing, CPAs are used because they have been shown to protect cells from freezing damage [26]. Vitrification methods attempt to prevent ice formation by promoting formation of a non-crystalline glassy state using high CPA concentrations. In either case, CPAs are a crucial component of the cryopreservation medium.

The process of adding and removing CPAs causes osmotic transport of water across the cell membrane, which can result in damaging changes in cell volume [14]. Even when excessive cell volume changes do not occur, exposure to CPAs can still cause cell damage because of toxicity. There is evidence that CPA toxicity reduces the efficacy of conventional freezing procedures in some cases [11], and problems with toxicity are even more pronounced in vitrification methods. In fact, overcoming CPA toxicity is widely considered to be the major challenge in the design of vitrification procedures [13].

Recently, two groups reported strategies for mathematically minimizing toxicity during CPA addition and removal [4,19]. Both strategies are based on the premise that the protocol with the shortest duration corresponds with the lowest toxicity. Karlsson et al. [19] used an iterative approach to minimize a cost equal to the duration of the CPA addition or removal process. They considered procedures with two step-changes in the extracellular solution composition, and excessive cell volume excursions were avoided by adding a penalty to the cost function when the predicted cell volume exceeded the osmotic tolerance limits. The

approach reported by Benson et al. [4] is similar, in that the objective of the optimization was to minimize the protocol duration subject to osmotic tolerance limits which were employed as cell volume constraints. However, Benson and colleagues did not limit their analysis to two-step protocols, and they used optimal control theory to determine the optimal protocol directly.

The degree to which toxicity causes damage during CPA addition and removal depends on several factors, including the CPA type, the duration of exposure to CPA, the CPA concentration and the temperature [8,10,12,13,21,36,37]. To effectively describe and subsequently minimize toxicity, each of these factors must be considered. As a result, identification of the optimal method for adding and removing CPA is a challenging problem. The mathematical strategies described above are based on the idea that minimizing the protocol duration is equivalent to minimizing toxicity. However, because toxicity is CPA concentration dependent, the shortest procedure may not minimize toxicity. To design minimally-toxic methods for adding and removing CPA, the effects of exposure time and concentration should be considered simultaneously.

In this study we introduce a CPA toxicity cost function, an equation that describes the accumulation of damage due to toxicity during CPA addition and removal. The cost function can be expressed in terms of the known factors affecting toxicity, including the CPA type, concentration and temperature. We focus here on the effects of CPA concentration on toxicity, and we describe a new strategy for mathematical optimization of CPA addition and removal procedures based on minimization of a concentration-dependent cost function. Using human oocytes as a representative cell type, we demonstrate that the procedures designed using this new optimization approach have the potential to dramatically reduce toxicity.

Materials and methods

Cell membrane transport model

Our basic strategy for optimizing CPA addition and removal procedures is based on minimizing a toxicity cost function while avoiding osmotic damage by keeping cell volumes constrained. The optimization approach makes use of predictions of cell membrane transport to evaluate the cost function, and to ensure that the cell volume does not violate the constraints. Transmembrane flux is proportional to the difference of chemical potentials, which is a function of the concentrations of solutes. The determination of the appropriate functional relationship has been debated in the literature and is challenging because most solution theories depend on measurement of mixture specific parameters [7,32]. Though a new theory has been proposed that addresses these concerns [7,9], flux rate parameters have not been measured in oocytes in the context of this formalism. Therefore, we will use the solute–solvent transmembrane flux model described by Jacobs [18] and commonly used in cryobiology [22] that provides an approximation of the difference in chemical potentials. We expect that the qualitative behavior of the optimal concentration functions should be reasonably independent of the chemical potential model, and with more experimental evidence supporting this new chemical potential formalism the direct numerical approach proposed in this manuscript will be easily adapted. After non-dimensionalizing the flux equations we have the system

$$\frac{dw}{d\tau} = -m_1 - m_2 + \frac{1+s}{w}, \tag{1}$$

$$\frac{ds}{d\tau} = b\left(m_2 - \frac{s}{w}\right),$$

where the non-dimensional variables are defined as in Katkov [20]: w is the intracellular water volume normalized to the water volume under isotonic conditions, s is the moles of intracellular CPA normalized to the moles of intracellular solute under isotonic conditions, τ is a dimensionless temporal variable, b is a unitless relative permeability constant, and m_1 and m_2 are the extracellular concentrations of non-permeating solute and CPA, respectively, normalized to the isotonic solute concentration. This model assumes that the cell behaves as an ideal osmometer during both shrinkage and swelling.

Cell volume constraints

In the cryobiological literature, the common assumption is that cells have a maximal and minimal total cell volume, beyond which cell death occurs [14,17,19]. The total cell volume consists of the volume occupied by intracellular water, the volume occupied by intracellular CPA, and the osmotically inactive volume (i.e., the portion of the cell volume that is not free to cross the cell membrane). In terms of the non-dimensional model, the total normalized cell volume can be defined as $v = w + \gamma s + v_b$, where γ is the product of the isotonic solute concentration and the partial molal volume of CPA, and the constant v_b is the osmotically inactive volume normalized to the cell water volume under isotonic conditions. If v_* and v^* are the minimal and maximal normalized cell volumes, respectively, we have the constraint that $v_* \leqslant v \leqslant v^*$, which we can also write as

$$v_* - v_b \leqslant w + \gamma s \leqslant v^* - v_b. \tag{2}$$

Toxicity cost function

Toxicity encompasses all damage associated with exposure to CPA that does not result from cell shrinkage or swelling. The mechanisms of CPA toxicity are poorly understood, but may be related to CPA-induced alterations in cytoplasmic organization, membrane properties or cell metabolism [16]. The purpose of the toxicity cost function is to represent the cumulative toxicity incurred during the CPA addition or removal process. Here we define the cost function in terms of a toxicity rate parameter, k, which is expected to be at least dependent on the CPA concentration, CPA type and the temperature at which the procedure is carried out. The cumulative toxicity can be determined from the time-integral of this rate parameter, namely,

$$J = \int_0^{t^f} k\,dt, \tag{3}$$

where t^f is the duration of CPA exposure. To use this cost function to guide design of CPA addition and removal procedures, it is first necessary to determine the toxicity rate parameter k. In the present study, we focus on the effect of CPA concentration on toxicity. Both Elmoazzen et al. [8] and Wang et al. [36] measured cell viability as a function of time after exposure to various Me_2SO concentrations. Elmoazzen et al. performed experiments with cartilage tissue, and modeled cell death after exposure to the Me_2SO solutions using a first-order rate equation:

$$\frac{dN}{dt} = -kN, \tag{4}$$

where N is the number of viable cells and $k > 0$ is the rate parameter. The rate parameter was assumed constant (for exposure to a given Me_2SO concentration), which results in

$$\frac{N}{N_0} = \exp(-kt), \tag{5}$$

where N_0 is the number of viable cells at $t = 0$. Elmoazzen et al. [8] fit this equation to their data to determine values of k for exposure to each of the different Me_2SO concentrations. Wang et al. [36] also
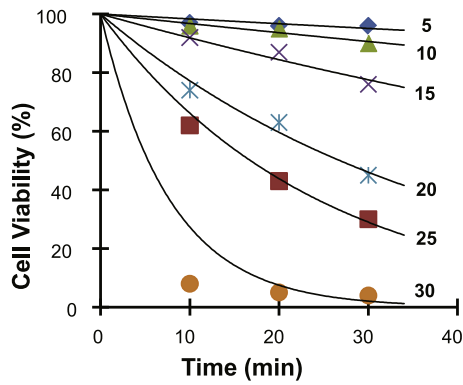
Fig. 1. Viability data reported by Wang et al. [36] for fibroblast cell suspensions after exposure to solutions with various Me₂SO concentrations at 25 °C (symbols). The lines show non-linear regressions to the data using Eq. (5). The Me₂SO concentration, in % v/v, is indicated to the right of each curve.
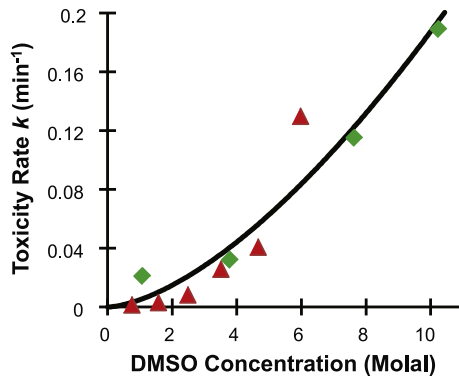
Fig. 2. Me₂SO toxicity rates at 22 °C from Elmoazzen et al. [8] (diamonds) and at 25 °C from Wang et al. [36] (triangles). The line shows the best-fit power function.

presented data that can be interpreted in terms of a first-order toxicity rate; their toxicity data for dermal fibroblast suspensions at 25 °C is shown in Fig. 1. We fit these data using Eq. (5) to determine best-fit values of k.

Fig. 2 shows the toxicity rates at 22 °C reported by Elmoazzen et al. [8], along with the rates that we determined using the data of Wang et al. [36]. Although these groups investigated different cell types, the toxicity rates follow a similar trend, with higher rates at higher Me₂SO concentrations. The concentration-dependence of the toxicity rate was well described by a power law relationship ($R^2 = 0.91$) with a best-fit function $k = 0.005(M_{2,i})^{1.6}$, where $M_{2,i}$ is the intracellular CPA molality (mol/kg). This concentration-dependence of toxicity is qualitatively consistent with published data for several different CPAs and for several different cell types [12,13,21]. Inserting this toxicity rate equation into the cost function results in

$$J = 0.005 \int_0^{\tau^f} (M_{2,i})^{1.6} dt. \tag{6}$$

Definition of the optimization problem

We wish to control the extracellular concentrations of permeating and non-permeating solutes (m_2 and m_1, respectively) such that cells are equilibrated at a goal state while minimizing the cumulative toxicity and avoiding excessive cell volume changes. To be precise, we wish to identify the trajectory between an initial state $x^i = (w^i, s^i)$ and a desired final state $x^f = (w^f, s^f)$ that minimizes

the cost function and avoids changes in the state variables w and s that exceed the constraints defined in Eq. (2). To permit expression of the cost function in terms of our non-dimensional variables, and in the interests of clarity, we define a simplified cost function based on the Eq. (6),

$$J_\alpha = \int_0^{\tau^f} m_{2,i}^\alpha d\tau = \int_0^{\tau^f} \frac{s^\alpha}{w^\alpha} d\tau, \tag{7}$$

where $m_{2,i}$ is the intracellular CPA molality normalized to the isotonic molality and $\alpha = 1.6$ is a constant describing the concentration-dependence of the toxicity rate.

Toxicity minimization strategy

We employed ALGENCAN [1,2], an implementation of a constrained optimization algorithm, to minimize the modified cost function

$$J_{\alpha,\varepsilon} = J_\alpha + J_\varepsilon, \tag{8}$$

where J_ε is a cost associated with the deviation between the actual final state $x(\tau^f)$ and the desired final state $x^f = (w^f, s^f)$, and is defined as

$$J_\varepsilon = \frac{1}{\varepsilon} \| x(\tau^f) - x^f \|^2 = \frac{1}{\varepsilon} ((w(\tau^f) - w^f)^2 + (s(\tau^f) - s^f)^2). \tag{9}$$

ALGENCAN uses a truncated-Newton approach to solve the resulting optimality system. It requires a numerical approximation of the Hessian-vector product to solve the augmented Lagrangian problem induced by the constrained optimization. With this type of optimization problem, "exact" controllability is known to be achievable [4]. This means there exist optimal controls such that the desired final state can be exactly reached. Note that as ε approaches zero, we approach "exact" controllability. In the interest of brevity, we only show numerical results for $\varepsilon = 10^{-3}$.

We parameterized the continuous functions $m_1(\tau)$ and $m_2(\tau)$ by dividing the temporal domain ($0 \leqslant \tau \leqslant \tau^f$) into 49 equally spaced linear segments. This corresponds with 50 bounded parameters for m_1 ($0 \leqslant m_1^j \leqslant \bar{m}_1$, $j = 1, \ldots, 50$) and 50 bounded parameters for m_2 ($0 \leqslant m_2^j \leqslant \bar{m}_2$, $j = 1, \ldots, 50$), where $\bar{m}_1$ and $\bar{m}_2$ are upper bounds on concentration. Given the initial conditions x^i and estimates for the parameters τ^f, m_1^j and m_2^j, we solve system (1) via an explicit Heun method and calculate the modified cost function (Eq. (8)). The constraints were defined as

$$g_1 := \frac{1}{\tau^f} \int_0^{\tau^f} \chi_{w + \gamma s + v_b - v^*} (w(\tau) + \gamma s(\tau) + v_b - v^*) \, d\tau \leqslant 0,$$
$$g_2 := \frac{1}{\tau^f} \int_0^{\tau^f} \chi_{v_* - w - \gamma s - v_b} (v_* - w(\tau) - \gamma s(\tau) - v_b) \, d\tau \leqslant 0, \tag{10}$$

where $\chi_a = 0$ for $a < 0$, $\chi_a = 1$ for $a \geqslant 0$, and $w(\tau)$ and $s(\tau)$ are the solutions of system (1) under the interpolated controls. This formulation of the constraints simply tallies total time when the constraints are exceeded.

Comparison with existing CPA addition and removal strategies

To provide context for our new toxicity minimization strategy, we also examined CPA addition and removal procedures designed using the conventional stepwise approach [14], as well as the time minimization approach described in Benson et al. [4]. The conventional stepwise strategy for designing CPA addition and removal procedures is based entirely on avoiding osmotic damage. In each step of the stepwise procedure, we chose the extracellular CPA concentration that was predicted by system (1) to cause the cell volume to reach but not exceed its volume limit, and we chose the exposure time that resulted in 90% equilibration. The non-permeating solute concentration in each step was calculated using

$m_1 = 1 + \gamma m_2$, which ensures that the cell volume approaches the isotonic volume after equilibration with the CPA.

The time minimization approach described in Benson et al. [4] is equivalent to minimizing the cost function shown in Eq. (7) using $\alpha = 0$, subject to the osmotic tolerance constraints given in Eq. (2). We determined the time-optimal controls analytically, as described in Benson et al., and we also determined time-optimal CPA addition and removal procedures using the numerical optimization strategy described above. This allowed validation of the numerically approximated optimal procedures against the analytical solution.

Optimization of procedures for human oocytes

As an example cell type of significant clinical relevance, we selected human oocytes, for which published parameter values are available [28–30] and are given in Table 1. We chose a molarity of 6 mol/L ethylene glycol (EG) as a target, which is consistent with EG concentrations used in published studies of oocyte vitrification [23,24]. Calculations were made using a maximal external EG concentration of 7.3 mol/L, which corresponds to $\bar{m}_2 = 41$, and a maximal external concentration of non-permeating solute (e.g., NaCl or sucrose) of $\bar{m}_1 = 41$. These concentration bounds were chosen (somewhat arbitrarily) to limit viscosity.

Relationship between the cost function and cell viability

The cost function J defined in Eq. (6) is based on a concentration-dependent toxicity rate that was determined using experimental data for cartilage tissue and dermal fibroblast suspensions during exposure to Me_2SO [8,36]. Cell viability can be calculated from the value of J by combining Eqs. (3) and (4), which results in

$$\frac{N}{N_0} = \exp(-J). \qquad (11)$$

For the purpose of optimizing EG addition and removal procedures for human oocytes, we defined a simplified cost function J_α (Eq. (7)), which has a value that is proportional to J (i.e., $J_\alpha = 310J$). The simplified cost function retains the concentration-dependence that was determined from the Me_2SO toxicity data for cartilage and fibroblasts, but not the magnitude of the toxicity rate. Because the concentration-dependence of the toxicity rate is consistent with the common observation that toxicity increases

as the CPA concentration increases, we expect the CPA addition and removal procedures designed using Eq. (7) to be reasonably accurate. However, there is considerable uncertainty in using Me_2SO toxicity data for fibroblasts and cartilage to approximate the magnitude of the toxicity rate for human oocytes during exposure to EG, which makes it difficult to obtain accurate estimates for cell viability. Nonetheless, we have calculated the cell viability using Eq. (11) for illustrative purposes.

Results

Stepwise CPA addition and removal procedures

Conventional stepwise CPA addition and removal procedures for human oocytes are shown in Figs. 3 and 4. To avoid excessive shrinkage during CPA addition, the concentration must be increased in 3 steps to achieve the desired final concentration of 6 mol/L (i.e., $m_2 = 30$). The oocytes achieve 90% equilibration in 6 mol/L EG at a time point of $\tau = 32.2$. The target intracellular state, which corresponds with complete equilibration in the 6 mol/L EG solution, is asymptotically approached but never reached. This deviation from the target final state can be quantified using Eq. (9), which yields $J_\varepsilon = 1130$ at the point of 90% equilibration. The toxicity cost function (Eq. (7)) was used to estimate the extent of damage due to toxicity, yielding the most substantial increase in toxicity in the final step, when the EG concentration was the highest. After 90% equilibration in 6 mol/L EG, the toxicity cost reached a value of $J_\alpha = 4280$.

Five steps are required to prevent excessive swelling during EG removal. Each step corresponds with a decrease in the extracellular EG concentration, and in the final step, the oocytes are exposed to isotonic EG-free medium. They achieve 90% equilibration in this isotonic solution at a time point of $\tau = 44.0$. At this point, the deviation from the target final state corresponds with $J_\varepsilon = 54$, and $J_\varepsilon < 1$ for $\tau > 46.5$. The value of the toxicity cost function increased most rapidly in the beginning of the removal process, and reached a plateau towards the end of EG removal. After 90% equilibration

Table 1
Definition of parameters for addition and removal of ethylene glycol for human oocytes.

Parameter	Parameter definition	Value
γ	Unitless partial molar volume	0.0168
b	Unitless relative membrane permeability constant	1.62[a]
$v^* - v_b$	Non-dimensional upper cell volume constraint	1.67[b]
$v_* - v_b$	Non-dimensional lower cell volume constraint	0.47[b]
w^i, s^i (Addition)	Initial values of non-dimensional variables for CPA addition	1, 0
w^f, s^f (Addition)	Final values of non-dimensional variables for CPA addition	0.67, 19.9
w^i, s^i (Removal)	Initial values of non-dimensional variables for CPA removal	0.67, 19.9
w^f, s^f (Removal)	Final values of non-dimensional variables for CPA removal	1, 0

[a] The value of b was calculated using permeability values at 22 °C from Mullen et al. [29].
[b] The lower and upper volume constraints were determined using data from Mullen et al. [28] and Newton et al. [30].
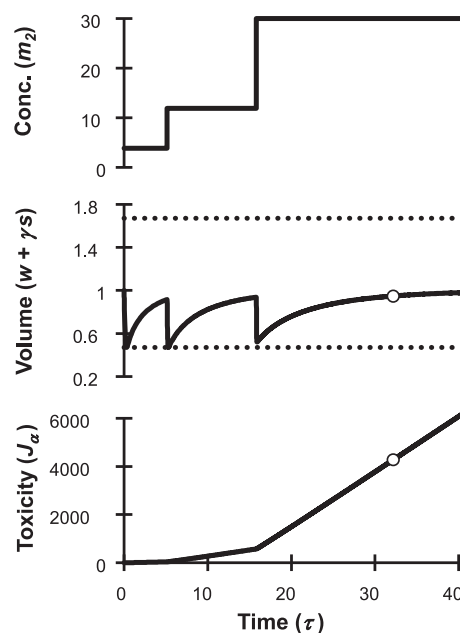
Fig. 3. Stepwise addition of 6 mol/L EG to human oocytes. Dotted lines show the osmotic tolerance limits and the white circles indicate 90% equilibration in the final 6 mol/L EG solution. The cumulative toxicity was calculated using Eq. (7) with $\alpha = 1.6$.
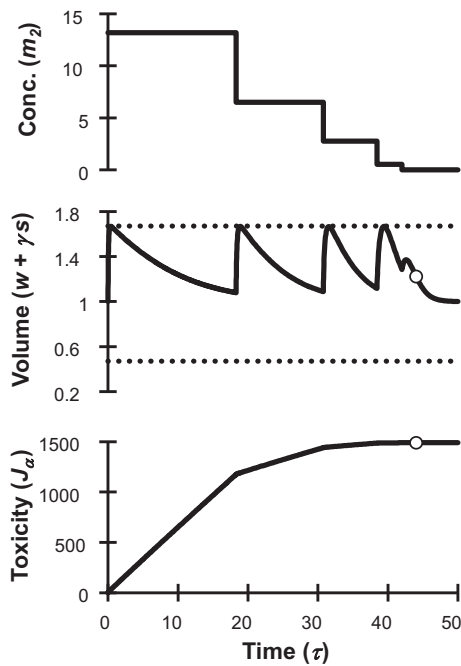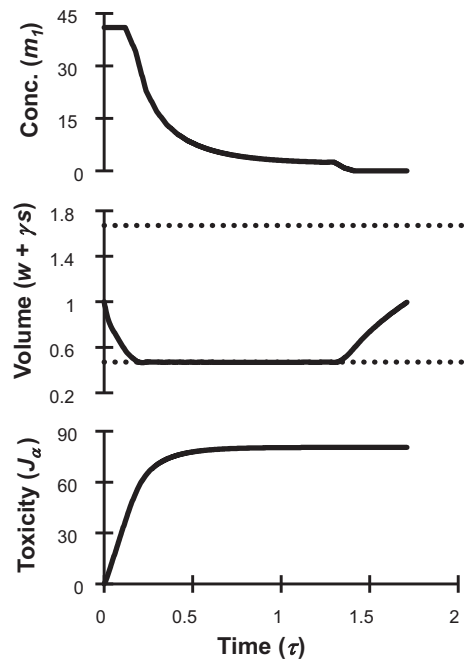
Fig. 4. Stepwise removal of 6 mol/L EG from human oocytes. Dotted lines show the osmotic tolerance limits and the white circles indicate 90% equilibration in the final EG-free solution. The cumulative toxicity was calculated using Eq. (7) with α = 1.6.

Fig. 6. Time-optimal removal of 6 mol/L EG from human oocytes. Dotted lines show the osmotic tolerance limits. The cumulative toxicity was calculated using Eq. (7) with α = 1.6.

in isotonic solution, the toxicity cost function reached a value of J_α = 1490.

Time-optimal CPA addition and removal procedures

CPA addition and removal procedures were also determined for human oocytes using the time minimization strategy described in Benson et al. [4] by numerically minimizing the cost function (Eq.

(7)) using α = 0. The results are shown in Figs. 5 and 6. As expected, from Benson and colleagues' previous analytical solution [4], the numerically optimized procedures yielded m_1 = 0 throughout the EG addition process and m_2 = 0 throughout the EG removal process, and both addition and removal procedures resulted in shrinkage to the minimum volume constraint. The numerically optimized procedures terminated near their target final states (J_ε < 3), and the procedures only deviated slightly from the previously defined analytical controls (not shown), validating our numerical approach.
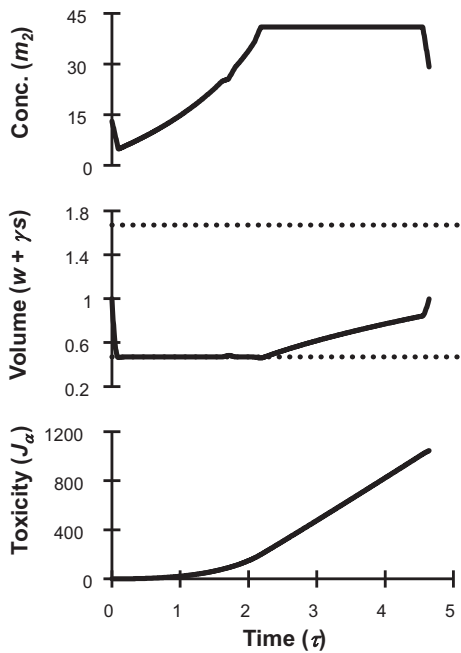
Fig. 5. Time-optimal addition of 6 mol/L EG to human oocytes. Dotted lines show the osmotic tolerance limits. The cumulative toxicity was calculated using Eq. (7) with α = 1.6.
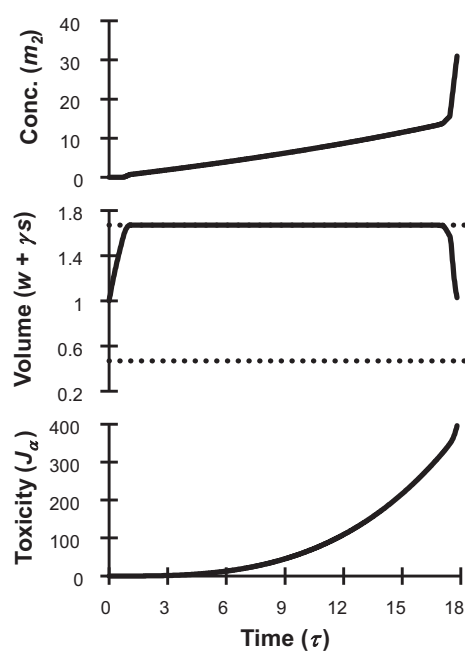
Fig. 7. Toxicity-optimal addition of 6 mol/L glycerol to human oocytes. Dotted lines show the osmotic tolerance limits. The cumulative toxicity was calculated using Eq. (7) with α = 1.6.

During addition, the toxicity cost reached a final value of $J_\alpha = 1050$ at a time point of $\tau = 4.7$. In the case of EG removal, the toxicity cost rapidly increased at the beginning of the procedure and then leveled out, reaching a final value of $J_\alpha = 80$ at $\tau = 1.7$.

Toxicity-optimal CPA addition and removal procedures

Fig. 7 shows the toxicity-minimal addition procedure for human oocytes, which consists of exposure to a time-varying EG concentration in the absence of non-permeating solutes (i.e., $m_1 = 0$). The EG addition process was completed at time $\tau = 17.8$, which is almost 4-fold longer than the time-optimal procedure, and the target final state was achieved nearly exactly ($J_\varepsilon < 4$). The toxicity reached a final value of $J_\alpha = 396$, more than 2-fold lower than that obtained using the time-optimal procedure, despite the fact that the time-optimal procedure is almost 4-fold shorter. Moreover, the cost of the toxicity-optimal procedure is an order of magnitude lower than that for conventional stepwise EG addition.

Fig. 8 shows the toxicity-optimal procedure for removal of 6 mol/L EG from human oocytes, which consists of exposure to EG-free solution containing a time-varying concentration of non-permeating solutes. The desired final state was reached almost exactly ($J_\varepsilon < 0.01$) at time $\tau = 5.3$, about 3-fold longer than the time-optimal removal procedure. The toxicity cost initially increased rapidly but reached a plateau at $\tau \sim 3$, after which J_α changed by less than 1%. As with the stepwise and time-optimal protocols, this suggests that for toxicity minimization, the critical portion of the removal procedure is the first half. After EG removal, the toxicity cost was $J_\alpha = 38$, more than 2-fold lower than for time-optimal removal and more than an order of magnitude lower than for stepwise removal. Moreover, the value of J_α for toxicity-optimal removal was more than 10-fold lower than for addition, indicating that toxicity is expected to be more pronounced during addition.

Oocyte viability estimates are shown in Table 2 for each of the different EG addition and removal procedures. The viability estimates were obtained using Eq. (11), which is based on the toxicity rate data in Fig. 2 for cartilage and fibroblasts during exposure to
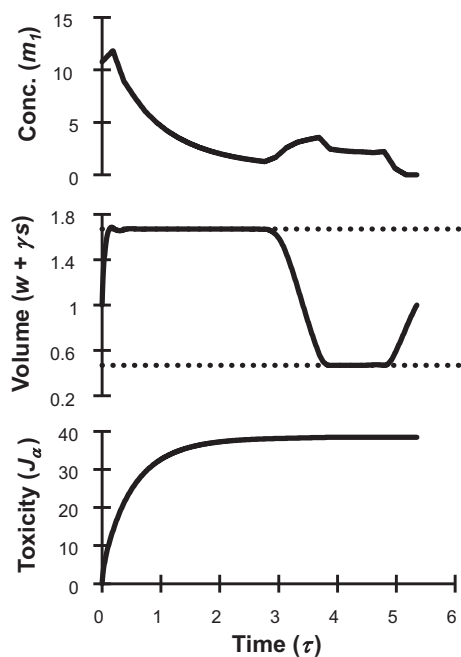
Table 2
Comparison of cell viabilities (%) estimated using Eq. (11).

	Toxicity-optimal	Time-optimal	Standard stepwise
CPA addition	28	3.4	10^{-4}
CPA removal[a]	89	77	0.8
CPA addition & removal	25	2.6	10^{-6}

[a] Assumes 100% viability prior to starting the removal process.

Me$_2$SO. As a result, the viability estimates for human oocytes during exposure to EG may be of limited accuracy. Nonetheless, it is still worthwhile to examine the viability estimates for the purpose of comparing the different CPA addition and removal strategies. The toxicity-optimal EG addition procedure is estimated to yield a cell viability of 28%, about eight times higher than the viability for time-optimal addition and more than 1000 times higher than the viability for stepwise addition. Toxicity-optimal removal is also estimated to yield a higher viability than the other removal strategies. Assuming an initial viability of 100% before initiating EG removal, the toxicity-optimal removal procedure is estimated to result in a viability of 89%, which is 1.2 times higher than the viability for time-optimal removal and more than 100 times higher than the viability for stepwise removal. If the entire EG addition and removal process is performed using the toxicity-optimal approach, it is estimated to yield a viability of 25%, whereas the time-optimal and stepwise approaches are estimated to yield a viabilities of only 2.6% and 0.000001%, respectively. Together, these results suggest that it may be possible to substantially improve cell viability using toxicity-optimal procedures.

Discussion

In the present study, we have developed a simple model for the kinetics of cell damage due to toxicity, and we have used this model to evaluate different strategies for designing CPA addition and removal procedures, with the ultimate goal of developing improved cryopreservation procedures. In particular, we have introduced a new strategy for designing procedures based on minimization of a toxicity cost function, a quantity that represents the damage due to toxicity accumulated during the addition or removal process. Our results provide several important insights about the factors affecting toxicity during CPA addition and removal.

Our new toxicity minimization strategy yielded a CPA addition procedure that was considerably different from the conventional stepwise approach. During toxicity-optimal CPA addition, the cells swell to their maximum tolerable volume, and they are loaded with CPA while in this swollen state. This result is counterintuitive because the ultimate goal of CPA addition is to equilibrate cells in highly hypertonic CPA solutions, and hypertonic solution is typically associated with shrinkage. In fact, the rationale for stepwise addition procedures is to prevent excessive shrinkage by increasing the CPA concentration in multiple steps. With our protocol, the cells are induced to swell using hypotonic solution and then maintained in the swollen state by increasing the CPA concentration gradually, such that the volume of water lost via osmotically driven flow is replaced by an equivalent volume of CPA entering the cells. In the final stage of the toxicity-optimal addition procedure, cell shrinkage is induced by exposure to a relatively high CPA concentration. This takes advantage of water efflux to quickly increase the intracellular CPA concentration at the end of the procedure. This strategy of concentrating intracellular CPA at the end of the addition procedure is similar to previous vitrification protocols presented in the literature. For instance, Rall and Fahy [33] reported successful vitrification of mouse embryos by first

Fig. 8. Toxicity-optimal removal of 6 mol/L glycerol from human oocytes. Dotted lines show the osmotic tolerance limits. The cumulative toxicity was calculated using Eq. (7) with $\alpha = 1.6$.

equilibrating the embryos in 3.3 mol/kg CPA solution, and then inducing shrinkage by exposure to 13 mol/kg solution directly before plunging into liquid nitrogen. Later reports by Steponkus et al. [35] and Mazur et al. [27] demonstrated vitrification of drosophila embryos using a similar approach. However, to the authors' knowledge, the potential for taking full advantage of swelling during CPA addition has not been investigated. The advantages of swelling can be demonstrated using the study of Rall and Fahy [33] as an example. Whereas Rall and Fahy equilibrated the cells in 3.3 mol/kg solution, the same *amount* of CPA could be loaded into swollen cells while maintaining a lower (and less toxic) intracellular CPA concentration. If, for example, we assume the cells tolerate swelling to twice their isotonic volume, the same amount of CPA could be loaded into the cells using a concentration of only 1.6 mol/kg.

The toxicity cost function developed in the present study also allowed comparison of the expected damage due to toxicity for different CPA addition and removal strategies. In general, CPA addition is expected to be associated with significantly more damage due to toxicity than CPA removal. The practical significance of this result is that it is important to carefully design and implement CPA addition procedures in order to minimize toxicity. The addition procedures designed using our new toxicity minimization approach are expected to significantly reduce damage due to toxicity compared with conventional stepwise procedures, as well as time-optimal procedures [4]. Thus, the new CPA addition approach that we have presented here has the potential to open new possibilities for cryopreservation using vitrification methods, where toxicity is often a major problem.

Although toxicity is expected to be less of a problem during CPA removal, it is still important to design removal procedures with toxicity in mind. Our results show that inducing swelling is beneficial because it decreases the intracellular CPA concentration and its associated toxicity, and that the use of CPA-free solutions is advantageous because it maximizes the driving force for CPA removal. The importance of this second effect is demonstrated by comparing the toxicity cost for time- and toxicity-optimal removal procedures (both of which involve exposure to CPA-free solutions) to the toxicity cost for stepwise removal (which involves exposure to solutions containing CPA). The toxicity- and time-optimal removal procedures drive the cell volume to the maximal and minimal limits, respectively. However, they both yielded toxicity costs an order of magnitude lower than for stepwise CPA removal, even though the cell volumes during stepwise removal also fall between the maximal and minimal limits. The critical difference is that both time- and toxicity-optimal procedures used CPA-free solutions. It is common in the literature to include CPA in the extracellular solution during CPA removal [6,31,33], but we are not the first to realize that using CPA-free solutions during removal may be advantageous [23,29].

Another important factor that will affect the damage due to toxicity incurred during CPA equilibration is the target final state, x^f. To compare different protocol design strategies we chose a consistent final state corresponding with complete equilibration in a 6 mol/L EG solution at isotonic volume: $x^f = (0.67, 19.9)$. For vitrification procedures, a final state is desired that permits vitrification of the intra- and extracellular solutions. This can be accomplished in several ways. For example, if we assume that 6 mol/L EG is a "vitrifiable concentration", an alternative strategy would be to use a final state corresponding with an intracellular EG concentration of 6 mol/L and a cell volume equal to the minimum volume limit (i.e., $s = 9.4$ and $w = 0.31$). If we re-run the optimization using this final state, the value of the toxicity cost function is reduced by about 8-fold to $J_\alpha = 48$, and the estimated viability is increased by about 3-fold to 86%. This demonstrates that simply choosing a different target state for CPA addition can have a dramatic impact on toxicity.

The applicability of our results depends on the accuracy of the toxicity cost function, which was generated using a limited set of published data on the toxicity of Me_2SO. We combined toxicity rate data from experiments on cartilage tissue [8] and fibroblast suspensions [36] and fit a power law model to the data, yielding an exponent $\alpha = 1.6$. This exponent was used in the cost function to estimate the damage due to toxicity incurred by human oocytes during addition and removal of EG. This analysis relies on the assumption that, in general, the concentration-dependence of toxicity can be described using a power law relationship with an exponent of $\alpha = 1.6$. A complete analysis of the effect of the value of α is beyond the scope of this study. However, we have examined optimal protocols with $1 \leqslant \alpha \leqslant 2$ and results were very similar (not shown).

Our results also rely on the assumption that osmotic damage can be avoided by using the osmotic tolerance limits as constraints on cell volume. Essentially, we have assumed that osmotic damage is negligible as long as the cell volume remains within the constraints. Others have suggested more complicated models for osmotic damage that take into account deviations from the isotonic cell volume, as well as the time over which these deviations occur [25]. This type of model could be incorporated into the cost function, allowing simultaneous minimization CPA toxicity and osmotic damage. To effectively implement this optimization approach, accurate quantitative models of both toxicity and osmotic damage are required. Further studies will be needed to obtain experimental data for development of such models.

We used mean values of published osmotic tolerance limits and membrane permeability parameters to predict optimal procedures, with the main goal of illustrating the efficacy of our new toxicity minimization approach. Because real cell populations exhibit a distribution of parameter values, the protocols presented here may not be effective for cells with properties that deviate substantially from the average. Given experimental data on the variability of cell properties, it would be possible to take into account the distribution of parameter values in the mathematical optimization scheme. However, this presents a new class of problem that is beyond the scope of the current manuscript.

We evaluated our new strategy for designing CPA addition and removal procedures using permeability data for human oocytes, so our results may have practical significance for oocyte cryopreservation. Over the last decade, there have been hundreds of investigations of human oocyte cryopreservation, and promising results have been reported using vitrification methods [3,5,23,24,38]. The most common approach is to initially expose cells to an equilibration solution with a low CPA concentration, followed by exposure to vitrification solution and ultra-rapid cooling in liquid nitrogen, a cooling protocol that is both technically challenging [3] and potentially non-sterile. Using methods described in the present study, it may be possible to safely achieve a higher final CPA concentration, which would relax the cooling and warming rate requirements for vitrification. This could lead to the development of facile vitrification procedures that use closed (sterile) containers, such as the commonly used freezing straws.

Conclusions

In this manuscript we have defined a new approach to the rational optimization of CPA addition and removal protocols based on minimization of toxicity cost function. We show that in the context of our cost measure, optimized protocols are significantly better than classically (and heuristically) defined "optimal" protocols. Our results open up many exciting avenues of future research. The most obvious next step is experimental validation of our optimized protocols. To implement the protocols it will be necessary to expose cells to time-varying solution compositions such as those

shown in Figs. 7 and 8. It may be possible to adapt previously reported microfluidic-based processes [15,34] for this purpose. The quantitative optimization approach presented here can generate not only new protocols, but also new biological and biophysical hypotheses that require experimental testing. To wit, the cost function reported in this study accounts for the effect of CPA concentration on toxicity, but does not account for the effects of temperature and CPA type. The development of a more complete cost function would enable mathematical optimization of the CPA type and temperature, factors that are currently only selected empirically. The numerical optimization framework will also be useful for investigating more complicated optimization problems. For example, coupling a cumulative cost of CPA addition with a cost of cooling and warming protocols (including the likelihood of lethal intracellular ice) would be a new and wholistic way to account for the complicated interactions between all parts of a cryopreservation protocol.

Acknowledgments

References

[1] R. Andreani, E.G. Birgin, J.M. Martinez, M.L. Schuverdt, On augmented Lagrangian methods with general lower-level constraints, Siam Journal on Optimization 18 (2008) 1286–1309.

[2] R. Andreani, E.G. Birgin, J.M. Martinez, M.L. Schuverdt, Augmented Lagrangian methods under the constant positive linear dependence constraint qualification, Mathematical Programming 111 (2008) 5–32.

[3] M. Antinori, E. Licata, G. Dani, F. Cerusico, C. Versaci, S. Antinori, Cryotop vitrification of human oocytes results in high survival rate and healthy deliveries, Reproductive Biomedicine Online 14 (2007) 72–79.

[4] J.D. Benson, C.C. Chicone, J.K. Critser, A general model for the dynamics of cell volume, global stability, and optimal control, Journal of Mathematical Biology 63 (2010) 339–359.

[5] A. Cobo, M. Kuwayama, S. Perez, A. Ruiz, A. Pellicer, J. Remohi, Comparison of concomitant outcome achieved with fresh and cryopreserved donor oocytes vitrified by the Cryotop method, Fertility and Sterility 89 (2008) 1657–1664.

[6] I.A.M. de Graaf, A.L. Draaisma, O. Schoeman, G.M. Fahy, G.M.M. Groothuis, H.J. Koster, Cryopreservation of rat precision-cut liver and kidney slices by rapid freezing and vitrification, Cryobiology 54 (2007) 1–12.

[7] J.A.W. Elliott, R.C. Prickett, H.Y. Elmoazzen, K.R. Porter, L.E. McGann, A multisolute osmotic virial equation for solutions of interest in biology, Journal of Physical Chemistry B 111 (2007) 1775–1785.

[8] H.Y. Elmoazzen, A. Poovadan, G.K. Law, J.A. Elliott, L.E. McGann, N.M. Jomha, Dimethyl sulfoxide toxicity kinetics in intact articular cartilage, Cell Tissue Bank 8 (2007) 125–133.

[9] H.Y. Elmoazzen, J.A. Elliott, L.E. McGann, Osmotic transport across cell membranes in non-dilute solutions: a new non-dilute solute transport equation, Biophysical Journal 96 (2009) 2559–2571.

[10] G.M. Fahy, Cryoprotectant toxicity – biochemical or osmotic, Cryo-Letters 5 (1984) 79–90.

[11] G.M. Fahy, The relevance of cryoprotectant toxicity to cryobiology, Cryobiology 23 (1986) 1–13.

[12] G.M. Fahy, T.H. Lilley, H. Linsdell, M.S. Douglas, H.T. Meryman, Cryoprotectant toxicity and cryoprotectant toxicity reduction: in search of molecular mechanisms, Cryobiology 27 (1990) 247–268.

[13] G.M. Fahy, B. Wowk, J. Wu, S. Paynter, Improved vitrification solutions based on the predictability of vitrification solution toxicity, Cryobiology 48 (2004) 22–35.

[14] D.Y. Gao, J. Liu, C. Liu, L.E. Mcgann, P.F. Watson, F.W. Kleinhans, P. Mazur, E.S. Critser, J.K. Critser, Prevention of osmotic injury to human spermatozoa during addition and removal of glycerol, Human Reproduction 10 (1995) 1109–1122.

[15] K.K.F. Glass, E.K. Longmire, A. Hubel, Optimization of a microfluidic device for diffusion-based extraction of DMSO from a cell suspension, International Journal of Heat and Mass Transfer 51 (2008) 5749–5757.

[16] R.H. Hammerstedt, J.K. Graham, Cryopreservation of poultry sperm: the enigma of glycerol, Cryobiology 29 (1992) 26–38.

[17] C.J. Hunt, S.E. Armitage, D.E. Pegg, Cryopreservation of umbilical cord blood: 1. Osmotically inactive volume, hydraulic conductivity and permeability of CD34(+) cells to dimethyl, sulphoxide, Cryobiology 46 (2003) 61–75.

[18] M.H. Jacobs, The exchange of material between the erythrocyte and its surroundings, The Harvey Lectures 22 (1927) 146–164.

[19] J.O.M. Karlsson, A.I. Younis, A.W.S. Chan, K.G. Gould, A. Eroglu, Permeability of the Rhesus monkey oocyte membrane to water and common cryoprotectants, Molecular Reproduction and Development 76 (2009) 321–333.

[20] I.I. Katkov, A two-parameter model of cell membrane permeability for multisolute systems, Cryobiology 40 (2000) 64–83.

[21] I.I. Katkov, N. Katkova, J.K. Critser, P. Mazur, Mouse spermatozoa in high concentrations of glycerol: chemical toxicity vs osmotic shock at normal and reduced oxygen concentrations, Cryobiology 37 (1998) 325–338.

[22] F.W. Kleinhans, Membrane permeability modeling: Kedem-Katchalsky vs a two-parameter formalism, Cryobiology 37 (1998) 271–289.

[23] L. Kuleshova, L. Gianaroli, C. Magli, A. Ferraretti, A. Trounson, Birth following vitrification of a small number of human oocytes: case report, Human Reproduction 14 (1999) 3077–3079.

[24] M. Kuwayama, G. Vajta, O. Kato, S.P. Leibo, Highly efficient vitrification method for cryopreservation of human oocytes, Reproductive Biomedicine Online 11 (2005) 300–308.

[25] J. Liu, S. Mullen, Q. Meng, J. Critser, A. Dinnyes, Determination of oocyte membrane permeability coefficients and their application to cryopreservation in a rabbit model, Cryobiology 59 (2009) 127–134.

[26] P. Mazur, Cryobiology: the freezing of biological systems, Science 168 (1970) 939–949.

[27] P. Mazur, K.W. Cole, J.W. Hall, P.D. Schreuders, A.P. Mahowald, Cryobiological preservation of drosophila embryos, Science 258 (1992) 1932–1935.

[28] S.F. Mullen, Y. Agca, D.C. Broermann, C.L. Jenkins, C.A. Johnson, J.K. Critser, The effect of osmotic stress on the metaphase II spindle of human oocytes, and the relevance to cryopreservation, Human Reproduction 19 (2004) 1148–1154.

[29] S.F. Mullen, M. Li, Y. Li, Z.J. Chen, J.K. Critser, Human oocyte vitrification: the permeability of metaphase II oocytes to water and ethylene glycol and the appliance toward vitrification, Fertility and Sterility 89 (2008) 1812–1825.

[30] H. Newton, D.E. Pegg, R. Barrass, R.G. Gosden, Osmotically inactive volume, hydraulic conductivity, and permeability to dimethyl sulphoxide of human mature oocytes, Journal of Reproduction and Fertility 117 (1999) 27–33.

[31] Y. Pichugin, G.M. Fahy, R. Morin, Cryopreservation of rat hippocampal slices by vitrification, Cryobiology 52 (2006) 228–240.

[32] R.C. Prickett, J.A. Elliott, S. Hakda, L.E. McGann, A non-ideal replacement for the Boyle van't Hoff equation, Cryobiology 57 (2008) 130–136.

[33] W.F. Rall, G.M. Fahy, Ice-free cryopreservation of mouse embryos at −196 °C by vitrification, Nature 313 (1985) 573–575.

[34] Y.S. Song, S. Moon, L. Hulli, S.K. Hasan, E. Kayaalp, U. Demirci, Microfluidics for cryopreservation, Lab on a Chip 9 (2009) 1874–1881.

[35] P.L. Steponkus, S.P. Myers, D.V. Lynch, L. Gardner, V. Bronshteyn, S.P. Leibo, W.F. Rall, R.E. Pitt, T.T. Lin, R.J. MacIntyre, Cryopreservation of *Drosophila melanogaster* embryos, Nature 345 (1990) 170–172.

[36] X. Wang, T.C. Hua, D.W. Sun, B.L. Liu, G.H. Yang, Y.L. Cao, Cryopreservation of tissue-engineered dermal replacement in Me₂SO: toxicity study and effects of concentration and cooling rates on cell viability, Cryobiology 55 (2007) 60–65.

[37] M.C. Wusteman, D.E. Pegg, M.P. Robinson, L.H. Wang, P. Fitch, Vitrification media: toxicity, permeability, and dielectric properties, Cryobiology 44 (2002) 24–37.

[38] T.K. Yoon, T.J. Kim, S.E. Park, S.W. Hong, J.J. Ko, H.M. Chung, K.Y. Cha, Live births after vitrification of oocytes in a stimulated in vitro fertilization-embryo transfer program, Fertility and Sterility 79 (2003) 1323–1326.